08,09

Effect of boron doping on luminescent properties of silicon–vacancy and germanium–vacancy color centers in diamond particles obtained by chemical vapor deposition

© S.A. Grudinkin[1], N.A. Feoktistov[1], K.V. Bogdanov[2], A.V. Baranov[2], V.G. Golubev[1]

[1] Ioffe Institute,
St. Petersburg, Russia
[2] Center of Information Optical Technologies, ITMO University,
St. Petersburg, Russia

E-mail: grudink.gvg@mail.ioffe.ru

Received June 14, 2022
Revised June 14, 2022
Accepted June 15, 2022

The effect of doping with boron on the luminescent properties of diamond particles synthesized by Hot Filament Chemical Vapor Deposition technique with color centers embedded during the growth process has been studied. It is shown that at low boron doping level, the photoluminescence intensity of a narrow zero-phonon line of the silicon-vacancy color center (738.2 nm) demonstrates a strong dependence on the concentration of boron atoms at the sites of the diamond lattice. The dependence of the intensity of a broad photoluminescence band in the wavelength range 520−800 nm on the concentration of boron atoms in the gas mixture in the range from 14 to 64000 ppm has been analyzed. The Raman scattering spectra of the obtained particles have been studied. At the concentration of boron atoms in the gas mixture up to 1540 ppm, the Raman scattering spectra of diamond particles practically do not change when the boron concentration is varied. At high boron doping level, the diamond band in the Raman spectra exhibit a spectral response typical of the Fano resonance.

Keywords: diamond particles, color centers, boron doping, photoluminescence, chemical vapor deposition.

DOI: 10.21883/PSS.2022.10.54243.405

1. Introduction

Doping of diamond with boron expands the prospects for applications of this unique in its physicochemical properties material [1–5]. When introduced into diamond, boron atoms are in the position of substitution of carbon atoms in the lattice, forming a deep acceptor level with an activation energy of 0.37 eV. When the concentration of boron is greater than $\sim 10^{20}\,\mathrm{cm}^{-3}$ there is a semiconductor–metal transition [6]. Boron-doped conductive diamond films are promising for creating an electronic component base for high-power electronics [2,4], for use as electrodes used in electrochemical processes [1,3], and as transparent conductive electrodes [5].

Due to the high value of the absorption coefficient, highly boron-doped diamond particles (DPs) can be used for local hyperthermia [7]. Nanodiamond particles obtained by chemical gas-phase deposition with introduced boron atoms are promising as a material for creating capacitors with a double electric layer [8]. Boron-doped diamond nanoparticles are used to create corrosion-resistant photoelectrocatalysts [9]. The use of boron-doped DPs as diamond nucleation centers for heteroepitaxial growth by chemical gas-phase deposition of conductive diamond films eliminates the presence of an insulating layer between the conductive diamond film and the substrate.

Boron Doping makes it possible to control the luminescence of optically active centers in diamond, for example, by changing their charge state [10–12]. Luminescent DPs with optically active color centers are of great interest as single-photon coherent radiation sources for quantum information science and luminescent markers for biomedicine [13]. For example, the work [11] demonstrated the possibility of using boron doping (at low concentrations of boron atoms — less than $2 \cdot 10^{17}\,\mathrm{cm}^{-3}$) to change the charge state of the silicon–vacancy color center from negative to neutral. The use of a sharp doping profile with a high concentration of boron atoms ($\sim 10^{20}\,\mathrm{cm}^{-3}\mathrm{nm}^{-1}$) leads to an increase in the concentration of vacancies in a positive charge state. This prevents the formation of divacancy complexes and allows to increase the characteristic time of spin coherence and the intensity of luminescence of the nitrogen–vacancy color centers in the negative charge state [12]. In the study [14] for selective heating of biological tissues and control of their temperature, it is proposed to use boron-doped nanodiamonds with nitrogen–vacancy color centers. Due to the temperature sensitivity of the energy of the transitions between the spin sublevels of the ground state of the center, they can act as an optical temperature sensor.

Promising functional material for biomedicine can be boron-doped DPs with introduced color centers of silicon–vacancy (SiV) and germanium–vacancy (GeV) in a negative

charge state. These centers are characterized by an intense and narrow zero phonon line (ZPL) of photoluminescence (PL), as well as low spectral diffusion of ZPL [13]. The centers consist of an internode atom, respectively, Si and Ge, as well as two nearby vacancies in neighboring lattice sites. Boron doping, leading to an increase in the absorption coefficient, will allow for effective heating of DPs with laser radiation, for example, during local hyperthermia and thermoablation therapy [7,14]. The possibility of using the high sensitivity of the shape and spectral position of the ZPL of the SiV and GeV color centers in boron-doped DPs for temperature control requires an analysis of the effect of boron concentration on the luminescent properties of these centers. Thus, for various applications, it is of interest to obtain DPs with introduced color centers and simultaneously doped with boron in a wide range of concentrations, as well as to study the effect of boron concentration on the structural and luminescent properties of the resulting particles.

The aim of this work was, firstly, to obtain boron-doped diamond particles with SiV and GeV color centers by hot filament chemical vapor deposition (HFCVD); secondly, the study by the methods of Raman spectroscopy of light scattering and photoluminescence spectroscopy of the influence of the content of boron atoms in a gas mixture in a wide range of concentrations on the optical properties of alloyed diamond particles. The choice of the HFCVD method is associated with a greater efficiency of boron injection due to the greater, compared to the MPCVD (Microwave Plasma Chemical Vapor Deposition) method, the lifetime of adsorbed boron atoms on the surface of the growing diamond crystallite in the synthesis process [15].

2. Experimental procedure

Boron-doped DPs are synthesized by HFCVD. Parameters of the HFCVD technological process: tungsten coil temperature — 2000–2200°C, operating pressure in the reactor — 48 Torr, hydrogen consumption — 480 sccm, methane concentration — 4%, diamond particle growth time — 3 h. Doping was achieved by introducing diborane (B_2H_6) into the gas mixture during synthesis. The ratio of the number of boron atoms to carbon atoms $(B/C)_{gas}$ in the diborane-methane mixture ranged from 14 to 64000 ppm.

Nanodiamonds of detonation synthesis with a characteristic size of ~ 4 nm were used as diamond nucleation centers [16]. The density of detonation fusion nanodiamonds deposited by aerosol spraying on the surface of the silicon substrate was $\sim 10^7\,cm^{-2}$. The size of the synthesized DPs, measured by atomic force microscopy, ranged from 0.9 to 1.5 μm. The source of the Si atoms was a substrate of crystalline silicon, and the source of atoms Ge — a plate of crystalline germanium located next to it on the substrate holder. During the synthesis process, solid-state sources of silicon and germanium were etched with atomic hydrogen, leading to the appearance of volatile radicals GeH_x and SiH_x. The transfer and deposition of radicals on the surface of growing DPs with the subsequent embedding of Ge and Si into the diamond lattice led to the formation of color centers.

The Raman scattering (RS) spectrum and PL were measured in the geometry of „backscatter“ using the Renishaw InVia micro-Raman spectrometer equipped with a confocal microscope. The spectral resolution of the spectrometer was $\sim 1\,cm^{-1}$. The wavelength of the exciting radiation was 488 nm. The excitation laser radiation was focused with a lens of $100 \times (NA = 0.9)$ in a spot on a sample with a diameter of $\sim 1\,\mu$m. PL spectra are measured at room temperature. Spectra of PL and RS were recorded from single isolated DPs.

3. Experimental results and discussion

The spectra of PL and RS of diamond particles obtained at low degrees of boron doping are shown in Fig. 1. The narrow band 602.3 nm in the spectrum of PL of undoped DP is the ZPL of the color center of GeV in the negative charge state. In spectra of undoped and doped DP at $(B/C)_{gas} = 46$ ppm there is an intense narrow ZPL of the color center of SiV in a negative charge state with a maximum at wavelength of 738.2 nm. With an increase in $(B/C)_{gas}$ there was a quenching of the ZPL centers of SiV and GeV.

In spectra *1* and *2* in Fig. 1 there are also weak narrow PL lines. Presumably, morphological defects localized on the twin boundaries or surface of diamond crystallites [17] are responsible for these narrow PL lines. In all these spectra of PL there is a wide band in the wavelength range of 520–800 nm. The origin of this band is due to optical

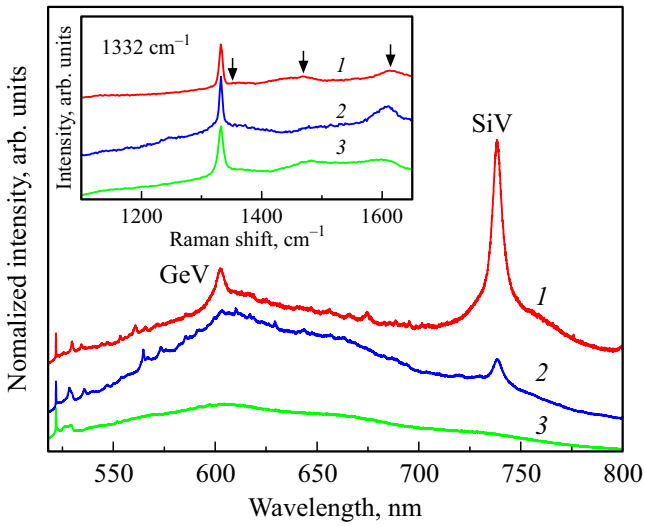

Figure 1. PL spectra of diamond particles obtained by the HFCVD method at the content of boron in a gas mixture $(B/C)_{gas}$: *1* — 0, *2* — 46, *3* — 1540 ppm. The spectra are normalized to the amplitude of the diamond RS line 521.9 nm. The insert shows the RS spectra of these particles.

transitions between continuously distributed energy states in the diamond band gap. These states are formed due to the presence of defects, for example, amorphous carbon with sp^2-hybridization of carbon bonds [18] or disordered sp^3-hybridized carbon [19]. Radiative recombination of donor-acceptor pairs [20] can also contribute to the observed broadband radiation.

In the PL spectrum of a diamond particle synthesized at $(B/C)_{gas} = 46$ ppm (Fig. 1, spectrum *2*), the wide PL band has two maxima at wavelengths of approximately 600 and 660 nm. The second maximum in its position is close to the band observed in the study [21] in the PL spectra of boron-doped diamonds synthesized at high pressures and high temperatures. The authors associate the appearance of this band with the recombination of donor-acceptor pairs, in which boron is an acceptor, and the donor can be, for example, nitrogen. The radiation of the centers of nitrogen–vacancy in the negative and neutral charge states, which have a wide band of phonon repetitions, can also contribute to the wide band of PL observed in the spectra [5].

The insert of Fig. 1 shows the RS spectra of diamond particles. In the RS spectra the band $\sim 1332\,cm^{-1}$ (diamond band) corresponds to the thrice-degenerate optical phonon symmetry mode F_{2g} in the center of the Brillouin zone in the diamond lattice and indicates the presence of a crystalline diamond phase in diamond particles (sp^3-hybridized carbon). For all RS spectra in the insert of Fig. 1, the width of the diamond band at half height (FWHM) is $\sim 7\,cm^{-1}$. Bands with maxima in the region of $1350\,cm^{-1}$ (D-line) and $1610\,cm^{-1}$ (G-line) are associated with the presence of sp^2-hybridized carbon in diamond particles. The band in the region of $1480\,cm^{-1}$ appears in the spectrum due to the presence of amorphous carbon in particles [22].

It was found that an increase in the degree of boron doping to tens of thousands of ppm leads to a significant change in the spectra of doped DPs — both PL and RS spectra. Typical spectra of PL and RS of DPs with a high degree of boron doping ($(B/C)_{gas} = 64000$ ppm) are shown in Fig. 2. Analysis of the RS spectrum given on the insert to Fig. 2 showed that Doping leads to a shift in the position of the maximum of the diamond RS band towards low frequencies ($\sim 1322\,cm^{-1}$) and its widening (FWHM $\sim 23\,cm^{-1}$). A comparison of the RS spectra of doped and non-doped DPs in the region of $1000-1550\,cm^{-1}$, shown in the inserts of Fig. 2 and Fig. 1, respectively, shows that at a high concentration of boron in the diamond lattice there is a strong change in the RS spectrum of the diamond particle, leading to the spectral response form typical for the Fano resonance [23–25]. The probable cause of resonance is the interaction of optical phonons (discrete phonon states) with free holes (continuum of electronic states). The continuum of electronic states is formed by excited states of acceptor levels and states in the valence band [23].

Analysis of the RS spectrum given on the insert to Fig. 2 shows that at high degrees of boron doping, there is a noticeable disorder of the crystal structure of DPs. In particular, intense wide bands appear in the spectrum with

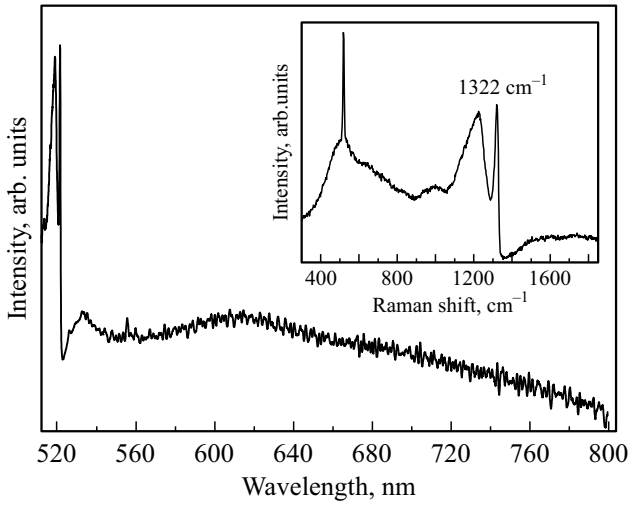

Figure 2. PL spectrum of a boron-doped diamond particle produced at $(B/C)_{gas} = 64000$ ppm. This insert shows the RS spectrum of this particle.

maxima in the region of 507 and $1220\,cm^{-1}$, the positions of which correspond to the maxima of the single-phonon density of the diamond states [26]. The emergence of these lines in the RS spectra becomes possible due to a violation of the rule of selection by the wave vector due to the appearance of defects in the diamond lattice at high concentrations of boron atoms in it. As a result, phonons from highly symmetric points of the Brillouin zone can contribute to the first order of RS spectrum [24,27]. Fano resonance also leads to a change in the shape of the band in the region of $1220\,cm^{-1}$ [24].

In the frequency range of $1350-1650\,cm^{-1}$ there is a wide structureless band, against which it is impossible to reliably distinguish the D- and G-bands. Perhaps due to the low intensity, these bands are not observed against the background of broadband PL. The observed wide structureless band in the RS spectrum is associated with the presence in the DPs with a high concentration of boron atoms of sp^2-hybridized carbon in the amorphous phase [28].

At the same time, with a high level of doping in the spectra, there is a noticeable decrease in the broadband PL signal in the region of $520-800$ nm, its intensity becomes significantly less than the intensity of the RS signal (spectrum *3* in Figs. 1 and 2). The cause of this effect requires more research; this may be due to the significant predominance of boron-induced defects over defects of other origins responsible for the formation of a wide PL band in the absence of doping. A more detailed analysis of the dependence of the intensity of broad PL on the concentration of boron is given below.

Note that in the RS spectra there are also RS band from a silicon substrate: a narrow intense band $520\,cm^{-1}$, due to the TO phonon mode of crystalline silicon, as well as a

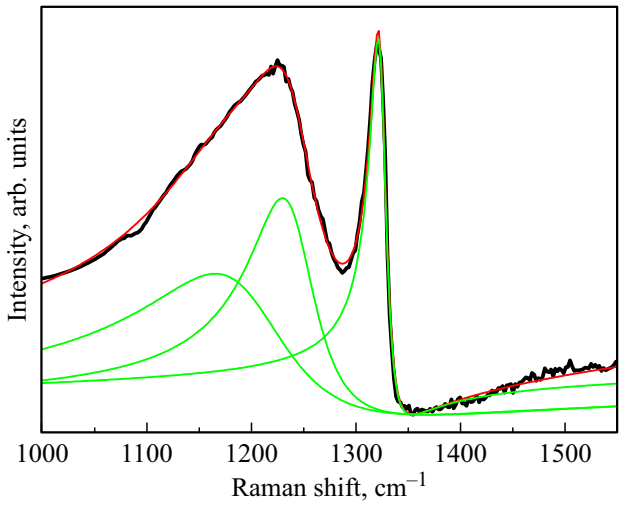

Figure 3. Experimental RS spectrum (black curve) and the results of the calculation using the Fano resonance model (red curve — fitting spectrum, green curves — individual RS band). Diamond particles are synthesized at $(B/C)_{gas} = 64000$ ppm.

wide band in the region of 940−1000 cm^{-1}, which is a RS band of the second order.

The spectral parameters (position and width) of RS bands depend on the concentration of boron in the diamond lattice at the substitution position [24,27]. Thus, the analysis of the RS spectra in highly doped boron diamonds is a way to estimate the concentration of boron atoms. To determine the spectral parameters of individual bands of RS, the decomposition of a typical experimental RS spectrum of a diamond particle obtained at $(B/C)_{gas} = 64000$ ppm (Fig. 3) was carried out. The decomposition took into account the contribution of the band of the optical phonon of diamond in the center of the Brillouin zone (~ 1332 cm^{-1}), as well as bands with maxima in the region of 1150 and 1220 cm^{-1}. The band in the region of 1150 cm^{-1} corresponds to an intense maximum of the single-phonon density of the diamond state [26]. Taking into account the contribution of this band in the decomposition of the spectrum makes it possible to adjust the experimental contour of a wide asymmetric band with a maximum near 1220 cm^{-1}. These bands ($i = 1, \ldots, 3$) were approximated by the Fano function [24]:

$$F_i(\nu) = \frac{1}{1+q_i^2}\,\frac{(q_i + (\nu-\nu_i)/\Gamma_i)^2}{1+((\nu-\nu_i)/\Gamma_i)^2}, \qquad (1)$$

where q_i — parameter that specifies the asymmetry of the path shape; ν_i — the position of the maximum band; Γ_i — parameter that describes the bandwidth.

The experimental spectrum is presented as a superposition of individual RS bands, taking into account the contribution of electronic RS due to the inelastic interaction of light with the continuum of electronic states, according to the method proposed in the work [29] for analyzing the spectra of boron-doped diamond RS. To determine the spectral parameters of individual RS bands, the calculation spectrum was adjusted to the experimental one. The selection of parameters is carried out by minimizing the standard deviation of the position of points on the theoretical RS spectrum from their position on the experimental spectrum. To find the minimum of standard deviation, the algorithm of differential evolution was used [30]. The values of spectral parameters obtained as a result of fitting are shown in the table.

The module of the parameter q, which determines the asymmetry of the RS band, is proportional to the ratio of the amplitude of light scattering on optical phonons to the scattering amplitude on free holes [25]. For undoped diamond particles $q \to \infty$. An increase in the probability of scattering on free charge carriers when doped with boron leads to a decrease in $|q|$. The negative values of the values q obtained as a result of the calculation reflect the observed asymmetry of the shape of the RS band [24,25]. The use of the dependence of the position of the maximum of diamond band on the concentration of boron obtained in the work [31] made it possible to estimate the concentration of boron atoms in the substitution position, which is equal to $\sim 1.1 \cdot 10^{21}$ cm^{-3} at $(B/C)_{gas} = 64000$ ppm.

It is known that the ZPL of the SiV center in diamond films and particles has a high intensity, regardless of the methods of gas-phase synthesis used, silicon doping methods and substrate materials [32–35]. This is due to the smaller size of the Si atom compared to the Ge atom, as a result of which it is more efficiently embedded in the diamond lattice to form an optically active center and is present in CVD diamond structures even at low content in the gas phase. Thus, when studying the effect of the entry of small concentrations of boron into the diamond lattice on the intensity of the ZPL of the color centers, it is preferable to analyze this dependence for the SiV center.

The dependence of the intensity of the ZPL of the SiV color center, normalized by the amplitude of the diamond RS band, on $(B/C)_{gas}$ in the range of 0−60 ppm is presented in Fig. 4. In this range, there is a strong decrease in the intensity of the ZPL of the SiV center with an increase in the boron content. The attenuation of the ZPL of SiV centers with an increase in the boron content occurs due to a decrease in their concentration due to the fact that boron atoms occupy the vacancies that are part of the centers [36]. Another possible reason for extinguishing the ZPL of the SiV center is a change in its charge state due to a shift in

The values of the spectral parameters of the diamond RS band, as well as the bands in the region of 1220 and 1150 cm^{-1} obtained as a result of fitting for diamond particles synthesized at $(B/C)_{gas} = 64000$ ppm

ν_1, cm^{-1}	Γ_1, cm^{-1}	q_1, cm^{-1}	ν_2, cm^{-1}	Γ_2, cm^{-1}	q_2, cm^{-1}	ν_3, cm^{-1}	Γ_3, cm^{-1}	q_3, cm^{-1}
1324.5	9.4	−3.1	1238.5	38.5	−3.3	1179.2	80.7	−2.1

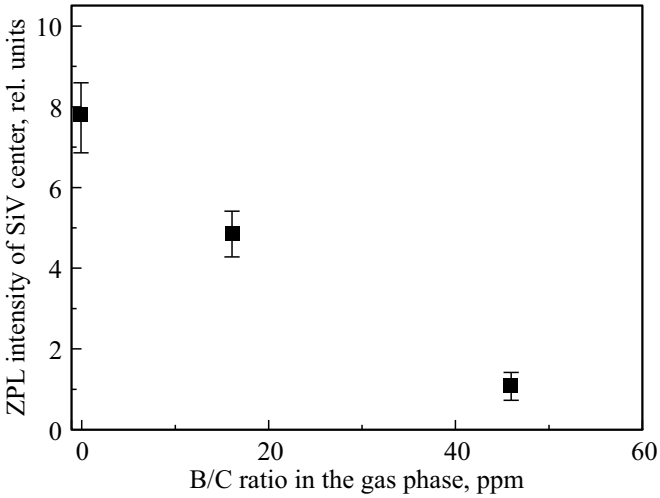

Figure 4. The dependence of the intensity of the SiV center ZPL on the concentration of boron in the gas mixture. The intensity of the SiV center ZPL is normalized to the amplitude of the RS of diamond line.

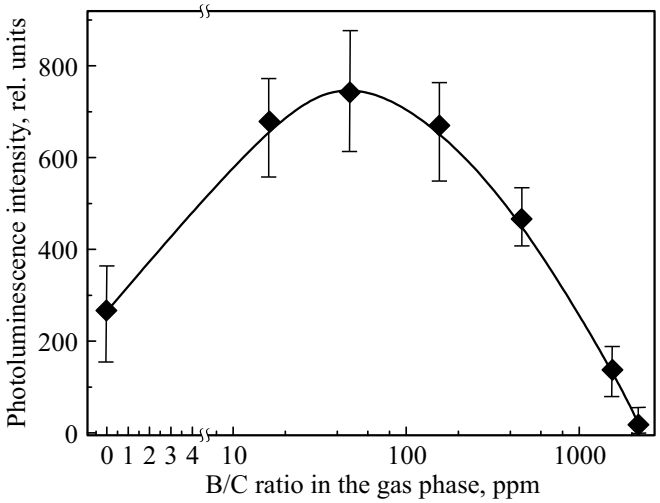

Figure 5. The dependence of the integral intensity of broadband PL on the concentration of boron in the gas mixture. The intensity of the PL is normalized to the intensity of the RS of diamond band.

the Fermi level position, in which it becomes energetically advantageous to form a silicon–vacancy center in a neutral charge state [11].

At $(B/C)_{gas}$ in the range of 0–46 ppm the RS spectra remain virtually unchanged (see insert in Fig. 1, spectra *1–3*). This is due to the fact that the concentration of boron atoms in the DPs is insufficient to form a continuum of states, the interaction with which optical phonons leads to a change in the shape of the spectrum of the RS of diamond. Thus, in this range of boron content in the gas phase, the analysis of the RS spectra does not make it possible to conclude that boron atoms enter the diamond lattice. In contrast, the intensity of the ZPL of the SiV color centers shows a strong dependence on the concentration of boron, which makes it possible to consider the color centers of the SiV as an indicator of the entry of boron into the lattice sites in weakly boron-doped diamond particles and films.

Figure 5 shows the dependence of the integral intensity of broadband PL on the concentration of boron in the gas mixture. The given intensity values are obtained by normalizing the intensity of the broadband PL by the intensity of the RS diamond band for each spectrum. The presented dependency has a maximum in the $(B/C)_{gas} = 46$ ppm region. The increase in the intensity of broadband PL is associated with an increase in the number of structural defects and the number of donor-acceptor pairs, leading to the appearance of energy states in the band gap. Extinguishing broadband PL with a further increase in the concentration of boron atoms in the diamond lattice may be the result of a decrease in the probability of radiative transitions between energy states in the band gap due to the activation of radiation-free recombination channels when embedding boron atoms into the lattice.

4. Conclusion

Boron-doped diamond particles with SiV and GeV color centers were synthesized by chemical gas-phase deposition with hot filament. The dependences of the intensities of the narrow ZPL of photoluminescence of the SiV center and broadband photoluminescence on the boron content in the gas mixture were studied. With a low content of boron in the gas mixture up to 1540 ppm the spectra of the RS of diamond band do not change. In the range from 0 to 46 ppm there is a strong extinguishing of the PL of the SiV color centers with an increase in the boron content in the gas mixture. With a low content of boron atoms, a change in the value of the intensity of the ZPL of the SiV center is a sensitive indicator that allows detecting the embedding of boron atoms into the sites of the diamond crystal lattice. The dependence of the intensity of broadband photoluminescence on the content of boron atoms in the gas mixture has a maximum at the value of $(B/C)_{gas} \approx 46$ ppm. In the highly doped particles, the shape of the RS bands corresponds to the asymmetric Fano contour.

Funding

The study was carried out using state budget funds on the topic of state assignment 0040-2019-0012.

Conflict of interest

The authors declare that they have no conflict of interest.

References

[1] S. Baluchová, A. Daňhel. H. Dejmková, V. Ostatná, M. Fojta, K. Schwarzová-Pecková. Anal. Chim. Acta **1077**, 30 (2019).
[2] X. Zhang, T. Matsumoto, S. Yamasaki, C.E. Nebel, T. Inokuma, N. Tokuda. J. Mater. Res. **36**, 1 (2021).
[3] C. Guo, J. Zheng, H. Deng, P. Shi, G. Zhao. Carbon **175**, 454 (2021).
[4] M.W. Geis, T.C. Wade, C.H. Wuorio, T.H. Fedynyshyn, B. Duncan, M.E. Plaut, J.O. Varghese, S.M. Warnock, S.A. Vitale, M.A. Hollis. Phys. Status Solidi A **215**, *22*, 1800681 (2018).
[5] M. Mermoux, B. Marcus, G.M. Swain, J.E. Butler. J. Phys. Chem. B **106**, *42*, 10816 (2002).
[6] T. Borst, O. Weis. Diam. Rel. Mater. **4**, *7*, 948 (1995).
[7] A.M. Vervald, S.A. Burikov, A.M. Scherbakov, O.S. Kudryavtsev, N.A. Kalyagina, I.I. Vlasov, E.A. Ekimov, T.A. Dolenko. ACS Biomater. Sci. Eng. **6**, *8*, 4446 (2020).
[8] K. Miyashita, T. Kondo, S. Sugai, T. Tei, M. Nishikawa, T. Tojo, M. Yuasa. Sci. Rep. **9**, *1*, 17846 (2019).
[9] L. Guo, V.M. Swope, B. Merzougui, L. Protsailo, M. Shao, Q. Yuan, G.M. Swain. J. Electrochem. Soc. **157**, *1*, A19 (2009).
[10] T. Lühmann, R. John, R. Wunderlich, J. Meijer, S. Pezzagna. Nature Commun. **10**, *1*, 4956 (2019).
[11] B.C. Rose, D. Huang, Z.-H. Zhang, P. Stevenson, A.M. Tyryshkin, S. Sangtawesin, S. Srinivasan, L. Loudin, M.L. Markham, A.M. Edmonds, D.J. Twitchen, S.A. Lyon, N.P. de Leon. Science **361**, *6397*, 60 (2018).
[12] F. Fávaro de Oliveira, D. Antonov, Y. Wang, P. Neumann, S.A. Momenzadeh, T. Häußermann, A. Pasquarelli, A. Denisenko, J. Wrachtrup. Nature Commun. **8**, *1*, 15409 (2017).
[13] C. Bradac, W. Gao, J. Forneris, M.E. Trusheim, I. Aharonovich. Nature Commun. **10**, 5625 (2019).
[14] M. Alkahtani, D.K. Zharkov, A.V. Leontyev, A.G. Shmelev, V.G. Nikiforov, P.R. Hemmer. Nanomater. **12**, *4*, 601 (2022).
[15] S. Ohmagari, M. Ogura, H. Umezawa, Y. Mokuno. J. Cryst. Growth. **479**, 52 (2017).
[16] N.A. Feoktistov, V.I. Sakharov, I.T. Serenkov, V.A. Tolmachev, I.V. Korkin, A.E. Aleksensky, A.Y. Vul, V.G. Golubev. ZhTF **81**, *5*, 132 (2011) (in Russian).
[17] V.G. Golubev, S.A. Grudinkin, V.Yu. Davydov, A.N. Smirnov, N.A. Feoktistov. FTT **59**, **12**, 2382 (2017) (in Russian).
[18] L. Bergman, M. McClure, J. Glass, R. Nemanich. J. Appl. Phys. **76**, *5*, 3020 (1994).
[19] S. Rahman, M. Othman, P. May. Adv. Mater. Res. **501**, 271 (2012).
[20] K. Fabisiak, W. Bala, K. Paprocki, M. Szreiber, C. Uniszkiewicz. Opt. Mater. **31**, *12*, 1873 (2009).
[21] P. Klein, M. Crossfield, J. Freitas Jr, A. Collins. Phys. Rev. B **51**, *15*, 9634 (1995).
[22] S. Prawer, R.J. Nemanich. Phil. Trans. R. Soc. Lond. A **362**, *1834*, 2537 (2004).
[23] J.W. Ager III, W. Walukiewicz, M. McCluskey, M.A. Plano, M.I. Landstrass. Appl. Phys. Lett. **66**, *5*, 616 (1995).
[24] V. Mortet, A. Taylor, Z.V. Živcová, D. Machon, O. Frank, P. Hubík, D. Trémouilles, L. Kavan. Diamond. Rel. Mater. **88**, 163 (2018).
[25] F. Pruvost, A. Deneuville. Diamond. Rel. Mater. **10**, *3–7*, 531 (2001).
[26] P. Pavone, K. Karch, O. Schütt, D. Strauch, W. Windl, P. Giannozzi, S. Baroni. Phys. Rev. B **48**, *5*, 3156 (1993).
[27] P. Gonon, E. Gheeraert, A. Deneuville, F. Fontaine, L. Abello, G. Lucazeau. J. Appl. Phys. **78**, *12*, 7059 (1995).
[28] J. Xu, Y. Yokota, R.A. Wong, Y. Kim, Y. Einaga. J. Am. Chem. Soc. **142**, *5*, 2310 (2020).
[29] V. Mortet, I. Gregora, A. Taylor, N. Lambert, P. Ashcheulov, Z. Gedeonova, P. Hubik. Carbon **168**, 319 (2020).
[30] R. Storn, K. Price. J. Glob. Optim. **11**, *4*, 341 (1997).
[31] V. Mortet, Z.V. Živcová, A. Taylor, M. Davydová, O. Frank, P. Hubík, J. Lorincik, M. Aleshin. Diamond. Rel. Mater. **93**, 54 (2019).
[32] A.A. Basov, M. Rähn, M. Pärs, I. Vlasov, I. Sildos, A. Bolshakov, V. Golubev, V. Ralchenko. Phys. Status Solidi A **206**, *9*, 2009 (2009).
[33] S.A. Grudinkin, N.A. Feoktistov, K.V. Bogdanov, M.A. Baranov, A.V. Baranov, A.V. Fedorov, V.G. Golubev. FTP **48**, *2*, 283 (2014) (in Russian).
[34] S.A. Grudinkin, N.A. Feoktistov, A.V. Medvedev, K.V. Bogdanov, A.V. Baranov, A.Y. Vul, V.G. Golubev. J. Phys. D **45**, *6*, 062001 (2012).
[35] V. Sedov, V. Ralchenko, A. Khomich, I. Vlasov, A. Vul, S. Savin, A. Goryachev, V. Konov. Diamond. Rel. Mater. **56**, 23 (2015).
[36] S. Dannefaer, W. Zhu, T. Bretagnon, D. Kerr. Phys. Rev. B **53**, *4*, 1979 (1996).